SYNTHESIS OF DIFFERENT MORPHOLOGICAL NANOSTRUCTURES OF TITANIUM DIOXIDE AND TO STUDY THEIR PHOTOCATALYTIC APPLICATIONS

A Thesis submitted

in partial fulfillment of the requirement for the award of the degree of

MASTERS OF SCIENCE

IN

CHEMISTRY

Under the supervision of

Dr. Bonamali Pal

Professor and Head, SCBC

Thapar University,

Patiala

Dr. Amjad Ali

Associate Professor, SCBC

Thapar University,

Patiala

Submitted By

Nishi Arora

Registration No.301302007

CERTIFICATE

This is to certify that the thesis entitled "Synthesis of different morphological nanostructures of titanium dioxide and to study their photocatalytic applications" being submitted in partial fulfillment of the requirement for the award of the degree of Masters of Science in Chemistry in the department of School of Chemistry and Biochemistry, Thapar University, Patiala is a bonafide work carried out under the supervision of Dr. Bonamali Pal, Professor and Head and Dr. Amjad Ali, Associate Professor, School of Chemistry and Biochemistry, Thapar University, Patiala and that no part of this project has been submitted for the award of any other degree.

Nishi Arora

(NISHI ARORA)

This is to certify that the above statement made by the student concerned is correct and true to the best of my knowledge.

(Dr. Bonamali Pal)
Professor and Head, SCBC
Thapar University,
Patiala

(Dr. Amjad Ali)
Associate Professor, SCBC
Thapar University,
Patiala

Countersigned By:

(Dr.Bonamali Pal)
Professor and Head, SCBC,
Thapar University,
Patiala, 147004

(Prof.(Dr).S.S.Bhatia)
Dean, Academic affairs,
Thapar University,
Patiala,147004

CANDIDATE'S DECLARATION

I hereby declare that the work presented in the thesis entitled, "Synthesis of different morphological nanostructures of titanium dioxide and to study their photocatalytic applications" being submitted in partial fulfillment of the requirement for the award of the degree of Masters of Science in Chemistry in the department of School of Chemistry and Biochemistry, Thapar University, Patiala, is an authentic work carried out under the supervision and guidance of Dr. Bonamali Pal, Professor and Head and Dr. Amjad Ali, Associate Professor, School of Chemistry and Biochemistry, Thapar University, Patiala and refers other researcher's work which are duly listed in the reference section.

The matter embodied in this thesis has not formed the basis for the award of any other degree of this or any university.

Date: July,2015
Place: Patiala

Nishi Arora.
(NISHI ARORA)

This is to certify that the above statement made by the student concerned is correct and true to the best of our knowledge.

(Dr. Bonamali Pal)
Professor and Head,SCBC
Thapar University,
Patiala

(Dr. Amjad Ali)
Associate Professor,SCBC
Thapar University,
Patiala

Acknowledgement

I would like to express my profound gratitude to my guides and mentors Dr. Bonamali Pal, Professor and Head, SCBC and Dr. Amjad Ali, Associate Professor, SCBC for their endless support throughout the tenure of my project. It is due to their priceless and effortless encouragement that paved the way for the successful completion of this work. I sincerely thank them for providing me affectionate encouragement and complete independence to explore and put my desire and thought into this project. It has indeed been a privilege to work under them.

I am indebted to my seniors and friends who have rendered all sorts of help and encouragement whenever and wherever required. I would take the opportunity to specially thank Mr. Rayees Ahmad, Mr Bhupender Pal, Ms. Abida Khan, Ms. Avneet Kaur, Ms Tanushree Basu for their consistent cooperation.

I would also thank all the teaching and non teaching staff for their invaluable cooperation and timely help through out the completion of my project.

A special thanks to my parents and brothers for being so patient and caring and always being available. Their love and belief in me is what makes me going.

I would be erring if I forget to thank my friends at Thapar University. It is through their kind gestures and beautiful company that I have been able to enjoy and love what I was doing. I am oblidged to Ms. Amanpreet, Ms. Gurjeet Kaur, Ms. Ritika, Ms Akansha for their courage, confidence and enthusiasm and moreover inspiration for hard work.

Lastly thank you God for making all things possible…

Date: July, 2015
Place: Patiala

Regards,
(Nishi Arora)
Nishi Arora.

Index

Contents Page No.

ABSTRACT

Nanoscience encompasses a wide range of applications and is the most advancing field these days. The small size range i.e, (10^{-9}) of these particles allows them to have efficient surface area and thus providing good catalytic properties. Several methods have been introduced for nanoparticle synthesis and have been industrially employed. Titania nanoparticles being an efficient semiconductor with low recombination rate have been widely studied. Its photocatalytic activity has been reported to be very high.

The present work demonstrates the synthesis of various morphologies of titania nanoparticles and its characterization along with its photodegradation properties. Its catalytic activity has been studied in the biodiesel synthesis. The degradation profile of salicylic acid using TiO_2 nanoparticles has been studied and the microwave synthesized titania nanoparticles proved to be excellent catalyst as compared to the conventionally synthesized and commercially available counterparts.

Chapter1

Introduction

The etymology of the word catalysis comes from ancient Greece, it basically means to accelerate the chemical reaction rate without the catalyst itself undergoing any change. This is done as the transition state lowers its energy and provides an alternative pathway for reaction. The catalysis reaction is of two types homogeneous, heterogeneous. Homogeneous is the catalysis where the catalyst exists in the same phase as that of the reactants, the basic disadvantage being the inability to completely recover the catalyst back from the reaction medium. The second type of catalyst include heterogeneous catalysis where the catalyst and the reactants aren't in the same phase, basic advantage of this type of catalyst is the easy isolation of the catalyst and its reusability. Considering a simple Haber process of nitrogen fixation, the catalyst used is finely powdered iron while the reactants are in gaseous phase. The yield is so high that it is industrially accepted for ammonia production.

1.1 Photocatalysis.

Photocatalysis, the type of catalysis reaction wherein the reaction is initiated in the presence of photons of light. Photocatalysis is a combination of two words photo derived from light and catalysis from catalyst. The substances which on light irradiation modify the reaction rate without undergoing any change are Photocatalysts. Semiconductors have been vastly employed as catalysts in heterogeneous photocatalysis, the semiconductor photocatalysis process occurs when a photon equal to or greater than band gap energy is absorbed, which results in the formation of excitons (electrons and holes). These charge carriers are responsible for the respective photooxidation and photoreduction of organic moieties. There are many examples of semiconductors as metal oxide, metal sulphides which are used as photo catalysts such as ZnO [1-2] , ZnS [3-5], TiO_2 [6-10], WO_3[11-12],etc. Semiconductors have a band gap in the range of visible and UV radiation and can therefore act as efficient photocatalysts.

1.2 Titanium dioxide (TiO_2):

TiO_2 being available in abundance, has low toxicity and high photocatalytic activity so is used as an efficient photocatalyst. Many applications of TiO_2 have been reported in recent years. It is widely used in mineralizing organic acids, organic pollutants, dyes, herbicides, etc. Basically

isolated from the ilmenite ore, titanium dioxide occurs in three phases namely rutile, anatase and brooklite. The anatase and brooklite states being metastable on heating from 600 to 800 ºC converts irreversibly to the rutile phase. Titanium dioxide being an efficient photocatalyst in the anatase form when doped with metal oxides such as MgO and ZnO functions under UV or visible light. The efficiency of the TiO_2 photocatalyst increases as the size and shape of the photocatalyst are tailored accordingly.

1.2.1. Mechanism of TiO_2 photocatalysis:

TiO_2 having a band gap of 3.2eV, a single particle absorbs a photon with energy higher than or equal to this band gap and can get easily excited from valence band to conduction band. This further stimulates the generation of a hole (h^+) and an electron (e^-) which results either in recombination and generation of heat or can react with other species. The holes can oxidize other species which can be depicted by the following equation:

$$TiO_2 + h\nu \rightarrow e^- + h^+$$

$$e^- + h^+ \rightarrow \text{heat}$$

$$h^+ + H_2O_{ads} \rightarrow \bullet OH + H^+$$

$$h^+ + OH_{ads} \rightarrow \bullet OH$$

$$\bullet OH + R \rightarrow CO_2 + H_2O$$

The electrons also react with the hydrogen peroxide and oxygen present in the solution. The electrons on reaction with oxygen gives superoxide or can form hydrogen peroxide on reaction with oxygen and hydrogen. On further reaction it can easily form hydroxyl radicals and hydroxyl ions. The reactions are as follows:

$$e^- + O_{2ads} \rightarrow O_2^-$$

$$2e^- + O_{2ads} + 2H^+ \rightarrow H_2O_2$$

$$e^- + H_2O_{2ads} \rightarrow \bullet OH + OH^-$$

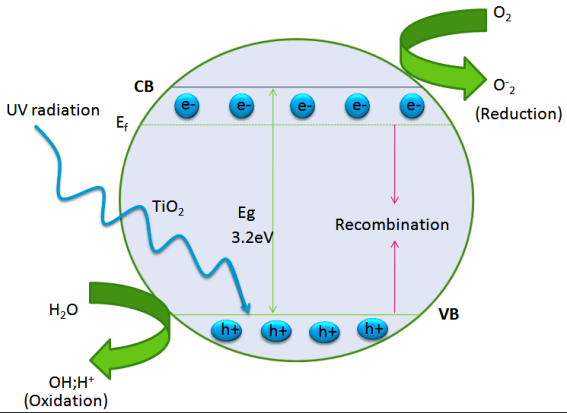

Figure1: Mechanism Of TiO_2 photocatalysis.

1.3 Titanium Dioxide in Biodiesel synthesis:

Biodiesels being an efficient environmental friendly alternative for the fuels can be synthesized using the mixed oxides of titanium dioxide and various other metals. Many reactions have been reported for the biodiesel synthesis esterification of acids and transesterification being the major two processes. The waste cooking oils[13], palm oil[14] and jatropha oil[15] have been commonly used for the biodiesel synthesis.

Chapter-2

Literature Survey

Titanium dioxide nanoparticles are versatile materials with their applications ranging from ointments, pigments, oils, paints, sunscreens etc. They have major applications in various fields such as photovoltaics, photoelectrochromics, sensors and photocatalysis. Many experiments have been reported for the synthesis and basic applications of titanium dioxide as catalyst. Xiaobo Chen and Samuel S. Mao[16] have effectively explained the various synthesis techniques along with the suggested modifications and applications. The direct impressions of the nanomaterials synthesized have been confirmed by scanning and transmission electron microscopy images. Sol gel synthesis where the sol, formed by the hydrolysis of inorganic metal salt precursors, micelle and inverse micelle methods, hydrothermal, solvothermal methods, microwave synthesis are few of the techniques reported and followed for the titanium dioxide nanoparticle synthesis.

Titanium dioxide has been employed in various photocatalytic activities, photodegradation being one of the major application. Various wastewater textile dyes have been effectively degraded using TiO_2 and its metal loaded components. Munusamy et al[17], studied the effect of dopants and compared its functionality with pure TiO_2. The dye used was brilliant green which showed an absorption maximum in the visible region (624nm). On further stirring with the TiO_2, Zn and Cu doped TiO_2 the various bands observed in various time intervals and the change in color is reported. Articles and publications have been reported where TiO_2 has been used in mineralization of organic acids such as malic and malonic acids. Vanessa et al[18] reported the photocatalytic degradation of malic acid using TiO_2 thin film and the mechanism has been reported, the thin film of TiO_2 prepared where quartz was used as base further different solutions of varying concentrations of malic and malonic acids were prepared and were detected using HPLC. It was then run in dark for an initial 30 minutes to reach adsorption equilibrium and then once the run was started the reaction was analyzed every hour to study the photocatalytic conversion of malic and malonic acid.

Further research explains the shape and size effect of the various nanoparticles of TiO_2 along with the effect of catalyst loading and dopant effect on various photodegradation processes as well as esterification and transesterification reactions. Due to more available surface area and

extended surface the titanium dioxide nanorods have higher photoactivity as compared to its nanospheres and the commercially available P25 counterparts. Asma et al[19] explains the different morphological and characterization properties and further used the synthesized catalysts in the degradation of formic acid. Using titanium dioxide P25 as reference the various titanium dioxide nanotubes and nanowires have been compared in properties and the adsorption studies have been reported.

Research has been continued to study the biodiesel production using titanium dioxide as catalyst. Usually mixed oxides are formed and are used in the biodiesel synthesis, Zhenzhong et al[20] have used waste cooking oil and catalyzed the reaction using titanium and magnesium mixed oxides in the synthesis of FAME with high reaction yield. They tried different Mg/Ti molar ratios and recorded maximum yield for Mg/Ti molar ratio of 1 i.e. 89.6%. They have studied different XRD patterns for various concentrations of Ti in the TiO_2-MgO mixed oxide and the trans-esterification reaction is studied.

2.1 Research gap:

Researchers have been keenly interested in studying TiO_2 nanoparticles because of its wide applications. Many reports have been made for various metal doped TiO_2 and its photocatalytic activity but bare TiO_2 and its activity based on its different morphologies has been very less reported. The nanosized TiO_2 rods which have elongated shape and higher surface area showing increased activity as compared to the nanospheres which have lesser surface area has been the subject of interest. The role of TiO_2 and the modifications done on its surface for the various photoreduction[21] and the role of the metal binders in their ability to increase reaction rate has been widely discussed. The detailed study on the TiO_2 nanostructures its various phases and their photochemistry, the various defects involved in the crystal system and their effect on the activity[22] mark an important area of interest. Owing to the various advantages of TiO_2 like high thermal stability, increased photocatalytic activity and abundant availability the TiO_2 has been advantageous for various studies. Thus every shape and size has its own uniqueness and can therefore influence the properties and activities of the nanoparticles to a large extent.

2.2 Objectives:

i) To synthesize titanium dioxide nanoparticles of different morphologies.

ii) Characterizations of the above synthesized nanoparticles by various techniques like UV, XRD, IR, EDX, SEM and TEM etc.

iii) To study its photocatalytic activity for degradation of salicylic acid and esterification reaction.

Chapter-3

MATERIALS & METHODS

3.1 Chemicals and Reagents:

The chemical and reagents used for this study were purchased from different sources and were used without any further purification. Titanium dioxide (TiO_2 P25) was a gift sample from Evonik Degussa, Germany. Titanium tetrachloride ($TiCl_4$, 99.5%), Polyethylene glycol (PEG), Hydrochloric acid (HCl) and Ammonium hydroxide (NH_4OH) were bought from Loba chemie, India. Salicylic acid (C_6H_4 (OH).COOH), acetic acid (CH_3COOH) and Titanium butoxide [$Ti(OBu)_4$] and ethylene glycol ($C_2H_6O_2$, 99%) were obtained from Spectrochem pvt ltd, India. Similarly acetone (CH_3COCH_3), methanol (CH_3OH, 99%) and Oleic acid ($C_{18}H_{34}O_2$) were purchased from S D fine Limited, India. All the synthesis was carried with deionised water obtained from ultra filtration system (Milli-Q, Milipore) with a measured conductivity (35 mho cm^{-1} at 25 ^oC).

3.2 Instruments used:

*3.2.1Microwave synthesizer***:**

Microwave synthesis of nanoparticles was carried out on Biotage microwave (Initiator$^+$EU) synthesizer with operating voltage of 220-240V, frequency of 50 Hz and power of 1100 Volt Amperes.

3.2.2 pH meter:

The pH of the solution during the TiO_2 nanorods synthesis was monitored using digital pH/conductivity meter (LMMP-30) from Labman Scientific Instruments Pvt. Ltd.

3.2.3 Magnetic stirrer:

Magnetic stirrer (REMI 2MLH) was used to maintain the titanium dioxide in suspension state to sought out the problem of aggregation during synthesis and the experiments.

3.2.4 Centrifugation Machine:

The washing and separation of synthesized photocatalyst was done with a centrifugation machine (REMI-R24). The separation and washing of catalyst was carried at 9,500-10,000 rpm at room temperature.

3.2.5 Photochemical Reactor:

All the photodegradation experiments were carried out under UV light irradiation mounted with an Hg vapor lamp source emitting (254 nm), power (125 W).

3.2.6 UV-Vis Spectrophotometer:

The photodegradation of salicylic acid in solution state was monitored using the Analytikjena Specord 205 and Perkin Elmer (Lambda 35) instrument in the wavelength region of 190 to 800 nm.

3.2.7 FTIR spectrophotometer:

The FTIR spectrum of catalyst and organic molecules were recorded in KBr pellet and ATR mode, respectively, using FTIR spectrophotometer (Cary-600).

3.2.8 Gas Chromatography (GC):

The CO_2 evolution of the reaction sample was determined by injecting the gaseous mixture into the gas chromatogram. The coloumn used is Propak-Q column, NUCON-5765 (30 mm × 0.32 mm × 12.00 μm). The carrier gas used was nitrogen (30 ml/min). The column temperature was set to be 50 ^{o}C while the injector and detector were set at 80 ^{o}C and 90 ^{o}C, respectively. The carrier gas used is nitrogen.

3.2.9 Scanning Electron Microscopy (SEM):

It was used to determine the surface morphology of the sample. The shape, size and surface topography was also confirmed by SEM. Instrument used was JSM7600F (0.1–30 KV)

3.2.10.Energy Dispersive X-Ray (EDX):

This technique was used to study the elemental composition of the selected areas of the sample. It was also helpful in identifying contaminants and their concentrations on the surface of the sample. EDX analysis was carried on JSM7600F.

3.2.10.BET:

The surface area of the powdered sample was analysed by BET surface area analysis. The instrument used Smartsorb 92/93 where the nitrogen adsorption desorption technique was used for the analysis of the porous surface at 77 K. During the analysis 100 mg of the sample were regenerated at 150 ^{o}C for 1 h.

3.3 Synthesis Of TiO_2 Nanoparticles:

3.3.1 Synthesis of microwave assisted sample of TiO_2 (Mw-TiO_2):

The microwave assisted titania nanoparticles were prepared by following the literature reported method [23] as shown in scheme 1. In a typical preparation, 2 g of polyethylene glycol was added to 48 g of HCl (0.5 M) and the solution was kept under vigorous stirring for 30 min. The transparent solution obtained was labeled as A. Simultaneously another solution (B) constituting of 3.78 g of titanium tetrachloride and 6 g dilute HCl (0.5 M) was kept under stirring for 30 min to obtain a pale yellow colored solution. Finally solution B was mixed with solution A and resulted solution was stirred for 30 min. The pH of the solution was maintained at 7 by adding dilute ammonium hydroxide to the solution. The resulted solution was further stirred for 1.5 h to obtain a colorless precipitates which was thoroughly washed with distilled water and kept in microwave synthesizer for 30 min. Then solid sample was isolated by centrifugation, calcined at 300 ^oC for 8 h and cooled to obtain white colored TiO_2 sample.

The scheme 1 clearly illustrates the process followed.

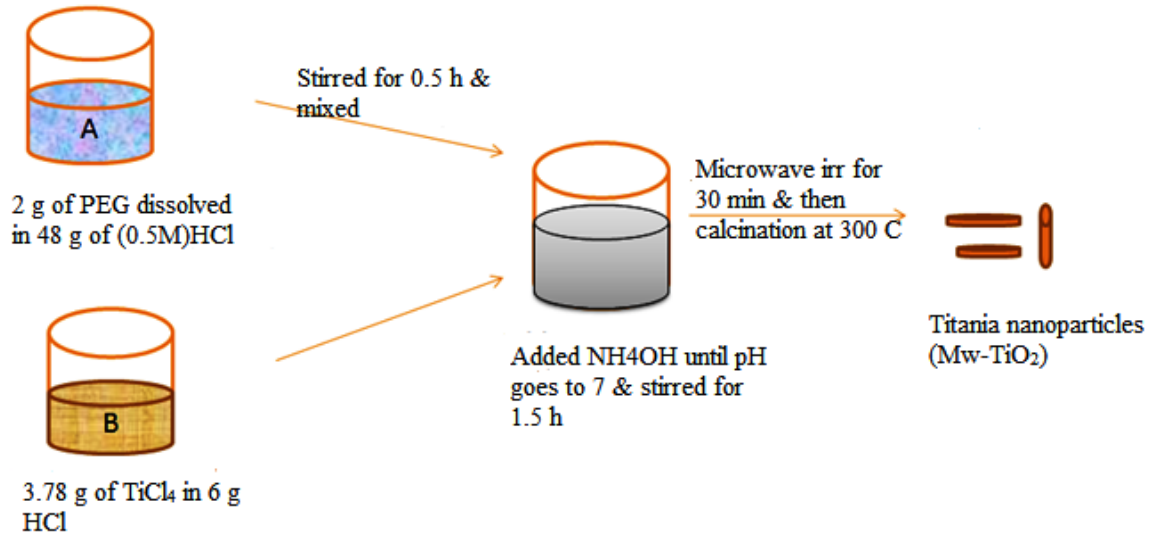

Scheme 1: Schematic representation for the synthesis of microwave assisted TiO_2 (Mw-TiO_2).

3.3.2 Synthesis Of template synthesised TiO_2 nanoparticles (Tw-TiO_2).

The preparation method followed for synthesis of titanium dioxide nanoparticles is as illustrated in Scheme 2 was as given by Damato et al[24]. In a typical preparation, 1 mL of titanium butoxide was added to 22.5 mL of ethylene glycol and prepared mixture was kept under vigorous stirring for 8 h at room temperature. The solution prepared was quickly poured into another solution of 100 mL of acetone, 1.25 mL of de-ionised water and 0.4 mL of acetic acid. The mixture obtained was then kept under vigorous stirring for 3 h at room temperature and then centrifuged at 10,000 rpm to obtain a white solid, which was successively washed several times with ethanol and water. Nanoparticles of titanium glycolate were stirred with 50 mL of water for 8 hours at 70 ºC to obtain a suspension. The precipitates was separated by centrifugation, dried and heated at 250 ºC for 2 h to obtain white coloured TiO_2 particles.

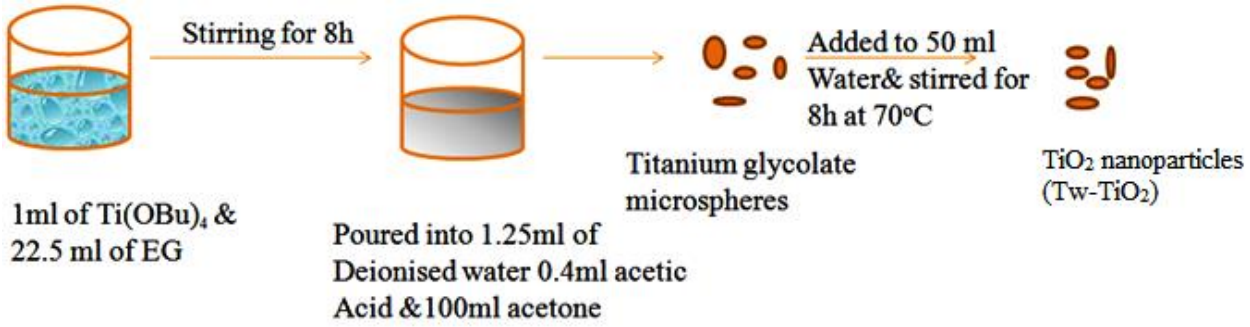

Scheme 2: Schematic representation of synthesis of Tw-TiO_2

3.4 Characterization of photocatalyst:

The prepared nanostructures of titanium dioxide (TiO_2 NR, TiO_2 NS, and TiO2 P25) were characterized by different optical and morphological techniques. The optical properties were analyzed by UV-Vis absorption spectrophotometer (Analytik Jena Specord-205, scan range 190-800nm) and Fourier transform infrared technique (Agilant, Cary 600) and the morphological characteristics were carried out by SEM-EDX(JSM 7600F) and TEM(Hitachi 7500) analysis. Further the crystal structure determination was done by X-ray diffraction. The specific surface area of the catalyst was analysed by BET surface area analyser.

3.5 Photocatalytic degradation of Salicylic Acid:

The comparative photocatalytic activity of TiO_2 nanoparticles is studied as a function of their shape. Herein we have studied the photocatalytic activity of Mw-TiO_2, Tw-TiO_2 and commercially available TiO_2 P25 for photodegradation of salicylic acid. A stock solution of 50 mL (0.2mM) salicylic acid ($C_7H_6O_3$) was prepared for the photocatalytic activity study. The photodegradation reaction was carried out in a test tube containing 5mL of stock solution and 20 mg of catalyst. Three separate test tubes labeled as T1, T2 and T3 were used for P25, Mw-TiO_2 and Tw-TiO_2 respectively. The photo mineralization reaction was carried out by continuous magnetic stirring under UV light for different time intervals. Further analysis of the reaction samples was done by UV-Vis spectrophotometer and FTIR spectroscopy. The scheme 3 represents the reaction process followed.

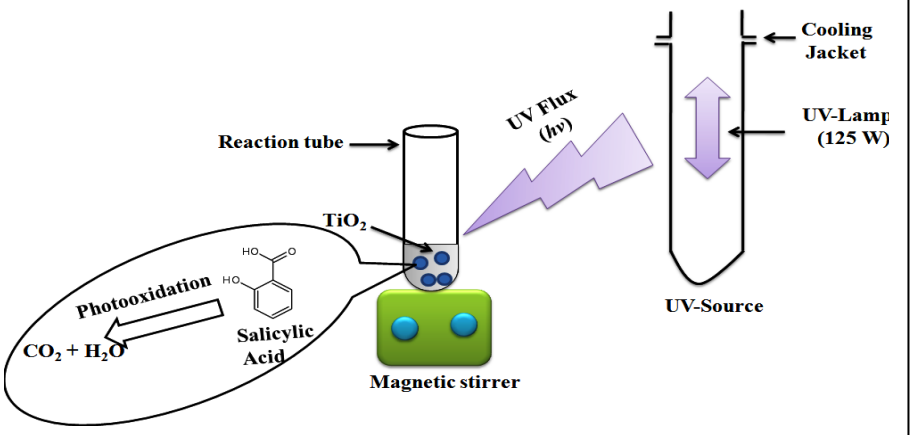

Scheme 3: Schematic representation of photochemical reaction set up and photodegradation of salicylic acid.

3.6 Esterification of Oleic Acid with methanol:

In a typical photocatalytic esterification reaction, the solution used was prepared with methanol and oleic acid (3:1 molar ratio). The catalyst concentration employed for the reaction was 15 wt% (with respect to oleic acid). In a typical reaction, 250 mg of appropriate catalyst (TiO_2 P25, Mw-TiO_2 and Tw-TiO_2) 1.87 mL of oleic acid and 0.702 mL of methanol were stirred for 7 h in a photochemical reactor. To monitor the progress of reaction the sample from the reaction

mixture was withdrawn after every 15 min by using a dropper, centrifuged to remove the catalyst and supernatant. The supernatant was diluted with hexane, and subjected to thin layer chromatography (TLC) using hexane/ethyl acetate (90:10, v/v) as the mobile phase and silica gel as stationary phase. Oleic acid and methyl oleate spots were used for the identification purpose. The product obtained was further characterized by comparing the FTIR peaks with the reference.

Chapter-4

Results & discussion

4.1 Optical properties of titania nanoparticles of different shapes:

4.1.1UV-vis analysis

The molecules when exposed to light in the UV (200-400nm) or visible (400-800nm) region can easily undergo electronic transition and the electron jumps from lower to higher energy state this is shown as absorbance peak. The optical absorbance of the photocatalyst was analysed by UV-Vis spectrophotometer (290-1100nm). The absorption maximum (λ_{max}) of synthesized Mw-TiO_2 and Tw-TiO_2 is illustrated in figure 2. The UV visible shows a λ_{max} at 310 nm for Mw-TiO_2 and at 342 nm for Tw-TiO_2 . The broader peak at absorption maxima is due to the discrete energy levels in the electronic structure of the TiO_2 nanoparticles.

The energy gap or band gap (E_g) was calculated by using the following mathematical formula;

$$\text{Band gap } (E_g) = 1240/\lambda$$

The band gap for Tw-TiO_2 and Mw-TiO_2 was observed at 3.9eV and 3.6eV, respectively which corresponds to their absorption in UV region while TiO_2 P25 shows a band gap of 3.2eV.

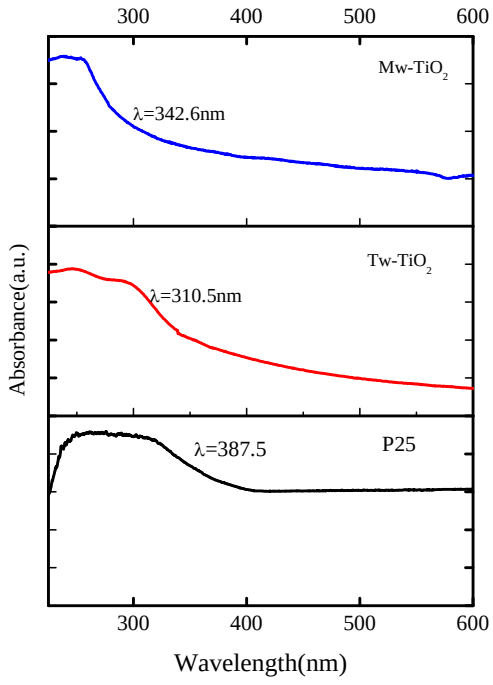

Figure 2: Absorbance spectra for various titania naoparticles.

4.1.2 FTIR characterization:

The functional properties of the surface of the photocatalyst were analysed by FTIR.

All the three samples were first made into KBr pellet and then mounted in the IR cell. The IR spectra was collected with a resolution of 4 cm^{-1} and 32 scans by a fourier transform infrared spectrophotometer.As shown in figure 3, a broad peak was observed in the 3000 to 3500 cm^{-1}

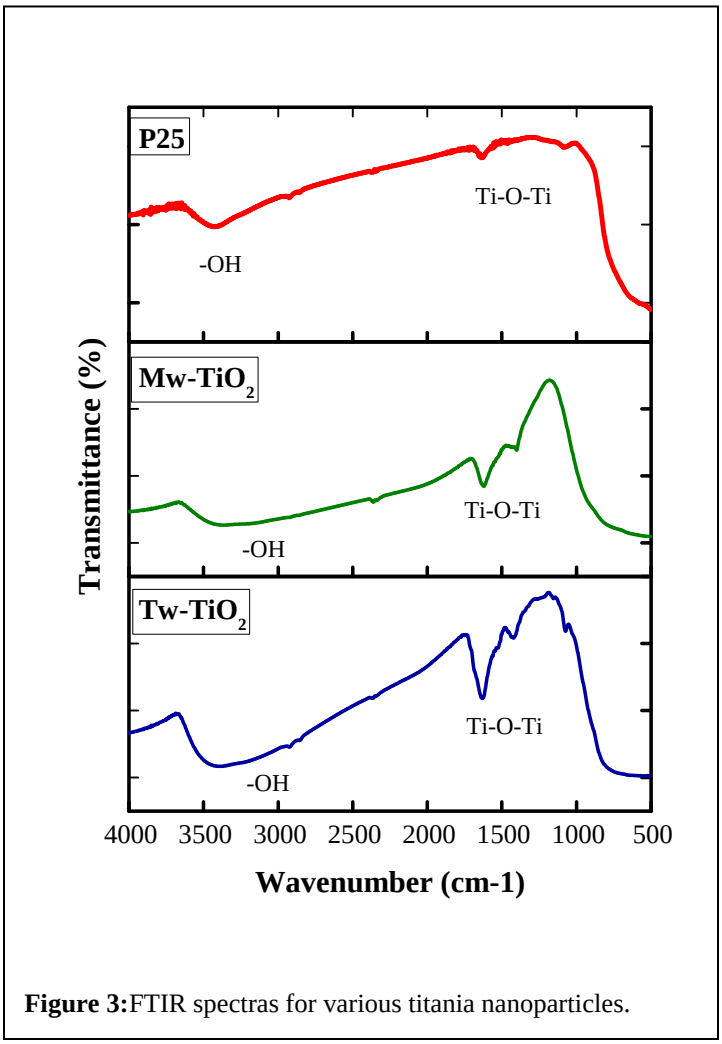

Figure 3:FTIR spectras for various titania nanoparticles.

region which is a characteristic peak for the associated hydroxyl group(–OH band) in all the three samples. These are attributed to the presence of monodentate hydroxyl group and bridging hydroxyl group which show stong interractions. These peaks are weakly chemisorbed and disappear as the temperature increases beyond 200 ^{o}C. Another sharp peak is observed at around 1500 to 1600 cm^{-1} which corresponds to the Ti-O-Ti band stretching and confirms the Titanium dioxide nanoparticles.

4.2 BET analysis:

The BET surface area (S_{BET}) analysis as shown in figure 4 shows higher surface area for Mw-TiO_2 (123.4 m^2/gm) and surface area for Tw-TiO_2 was observed as 46.4 m^2/gm. The specific surface area for TiO_2 P25 is 50.0 m^2/gm. The higher surface area for Mw-TiO_2 explains the higher photoactivity compared to that of the Tw-TiO_2 , while the photoactivity of commercially available TiO_2 P25 lies in between the two samples.

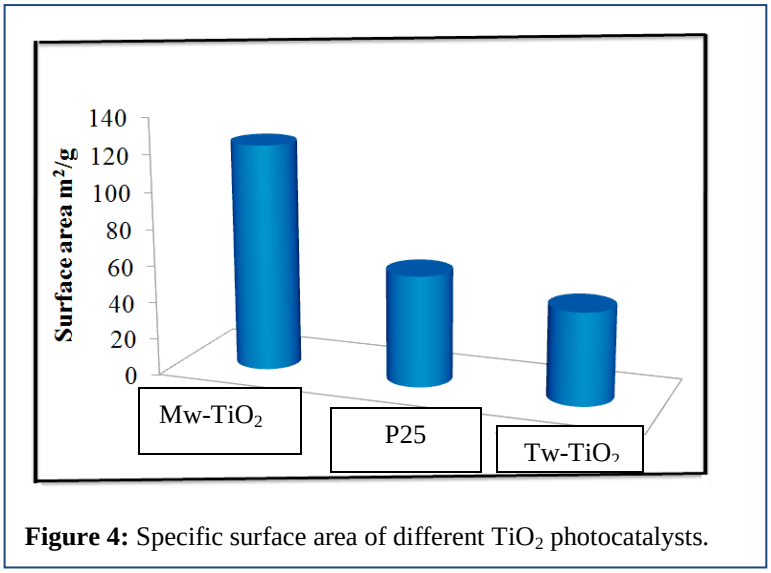

Figure 4: Specific surface area of different TiO_2 photocatalysts.

4.3 Morphological characterization:

4.3.1 XRD analysis:

The XRD patterns for the different Titania nanoparticles are shown in the figure 5. The Tw-TiO_2 synthesized by the template process shown in figure 5 shows 2Θ =25.4º peak which confirms anatase phase. The phase is further confirmed by comparing the anatase and rutile peaks with the TiO_2 P25 and both Mw-TiO_2 and Tw-TiO_2 show anatase peaks while the rutile peaks are absent. The Scherrer's equation estimates the average crystallite size of TiO_2 nanoparticles by the equation;

$$D = K\lambda/\beta\cos\theta$$

Where λ is the X ray wavelength, β is the peak width of half maximum, K is the Scherrer's constant and θ is Bragg's diffraction angle. The crystallite size as calculated by the Scherrer equation is 10.1nm for the Tw-TiO_2 which is in close agreement with the data from literature [24]. While Mw-TiO_2 shows crystallite size of 8.2 nm which holds good as compared with the size reported [23].

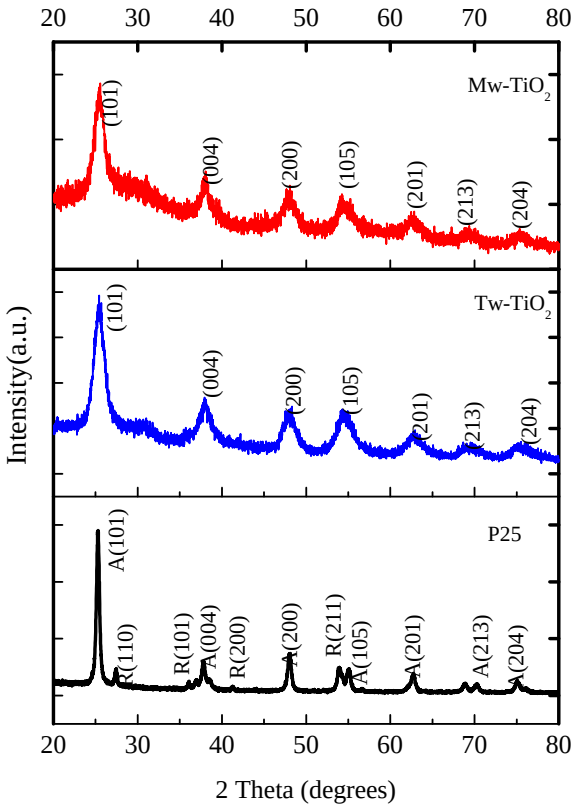

Figure 5: XRD patterns for various titania nanoparticles.

4.3.2. Energy dispersive X-ray spectrophotometer (EDX):

The chemical composition of the selected area of the sample was determined by EDX. The EDX spectra of Mw-TiO_2 confirms the presence of corresponding titania and oxygen elements with the atomic concentration as shown in the inset of figure 6. The element ratio table given in figure 6 shows the presence of large amount of carbon which is due to the pollution caused by the electrically conducting adhesive used during the EDX analysis.

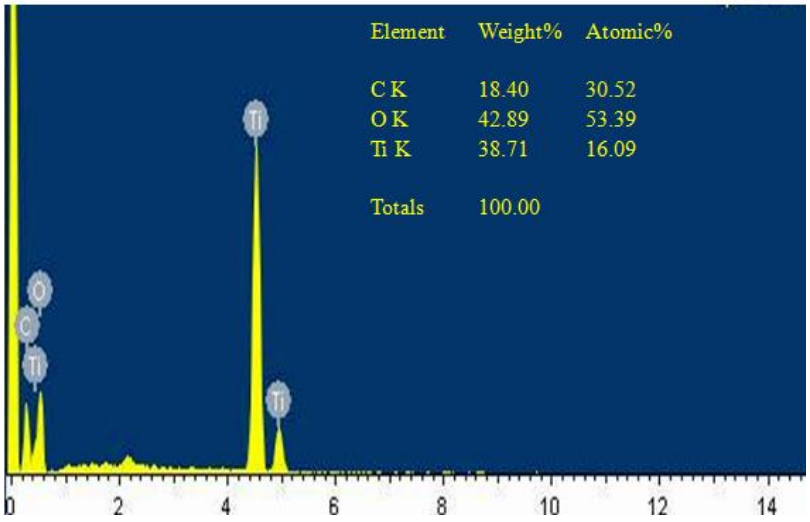

Figure 6: EDX spectrum of Tw-TiO_2.

Similarly, figure 7 shows the element content of the Mw-TiO_2. The EDX analysis confirms the titanium to oxygen atomic content to be almost half as suggested by its formula unit. The inset provides the element distribution ratio.

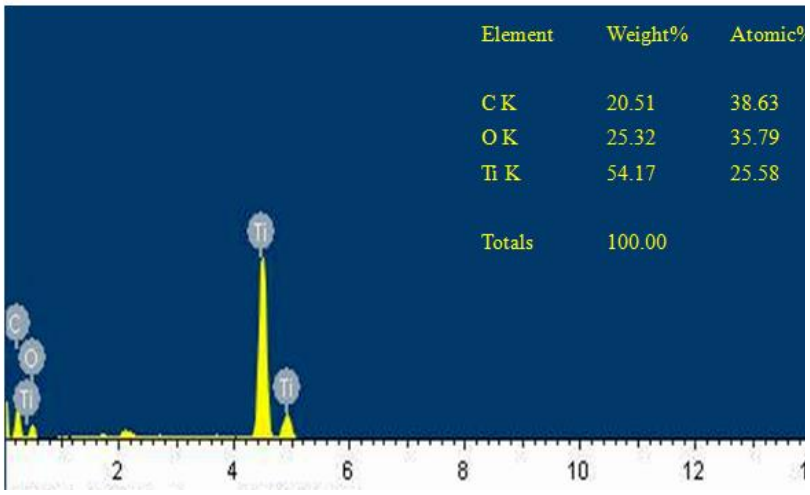

Figure 7: EDX spectrum of Mw-TiO_2.

4.3.3 Scanning Electron Microscopy (SEM):

The surface morphology of the sample was confirmed by SEM analysis. It showed spherical shape for the Tw-TiO_2 while the Mw-TiO_2 were clustered and elongated as shown in figure 8. The figure 8 clearly depicts the surface topography of the titania nanoparticles.

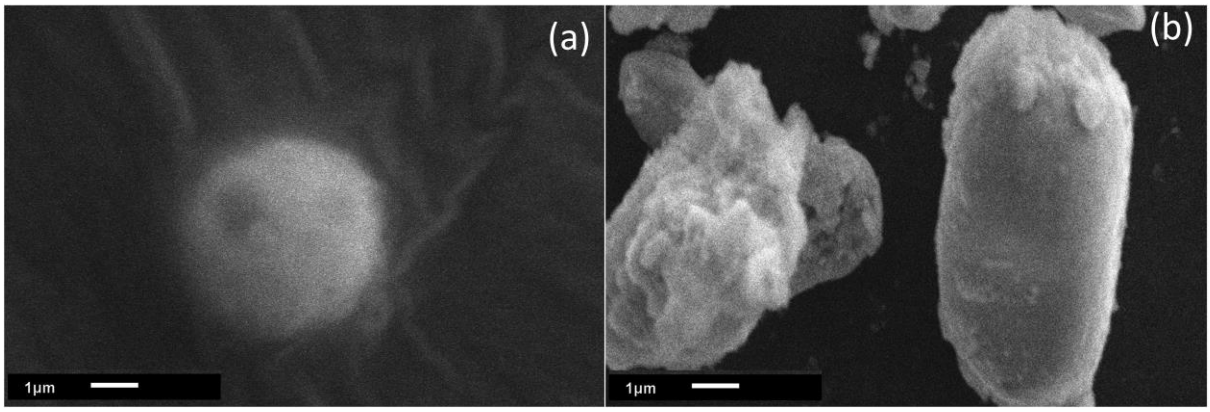

Figure 8: SEM images Of (a) Tw-TiO_2 and (b) Mw-TiO_2

4.3.3TEM:

The morphology of titania nanoparticles was confirmed by transmission electron microscopy (TEM). It confirms that TiO_2 P25 consists of a mixture of non spherical nanoparticles. The figure 9 clearly shows that the sample (a) is TiO_2 P25, (b) is Tw-TiO_2. The TEM images elucidates the sizes to be 50 nm for P25 nanoparticles while the Tw-TiO_2 are 10 nm in size.

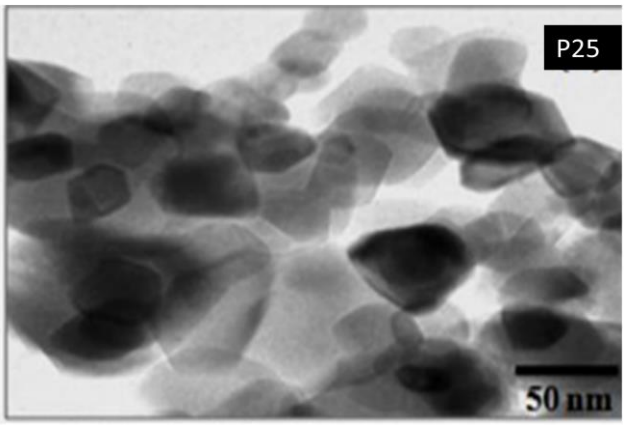

Figure 9: TEM image for P25

4.4 Photodegradation of salicylic acid:

The UV-vis spectrophotometry was used to analyse the amount of unreacted sample (salicylic acid) left in the reaction mixture. It used to realize the disappearance of a specie with reaction or the formation of new ones which would absorb in the UV region. The figure 10 gives the baseline corrected UV graphs at different time intervals for the degradation of salicylic acid. It follows the general trend of degradation on exposure to UV irradiation and leads to decrease in concentration of the acid solution.

4.4.1 Photolysis:

To monitor the independent light bleeching effect on salicylic acid 5ml of salicylic acid (0.02 mM) was irradiated in UV radiation without any catalyst. The sample was then studied for any change in the concentration by the UV-vis spectrophotometer at different time intervals (20,40, 60mins). No concentration change was observed with course of time.

4.4.2 Dark adsorption:

Dark adsorption studies have been carried out to study the adsorption desorption equilibria on the surface of catalyst. In general the heterogeneous catalysis follows Freundlich and Langmuir adsorption isotherms. It supports the study that the adsorption occurs at different energy sites and also supports the heterogeneity of the surface and it suggests that the adsorption varies as the fuction of surface coverage. The mathematical expression for multilayer adsorption as given by the Freundlich equation is given as:

$$x/m = Kc1/n \text{ or } \log x/m = \log K + 1/n \log C$$

where m being the mass of adsorbent, x is mass of adsorbate and c is the equilibrium concentration of adsorbate in solution k and n are constants at a given temperature for a particular combination of adsorbate and adsorbent. At higher concentration, $1/n \rightarrow 0$ and the adsorption extent becomes concentration independent following zero order reaction kinetics.

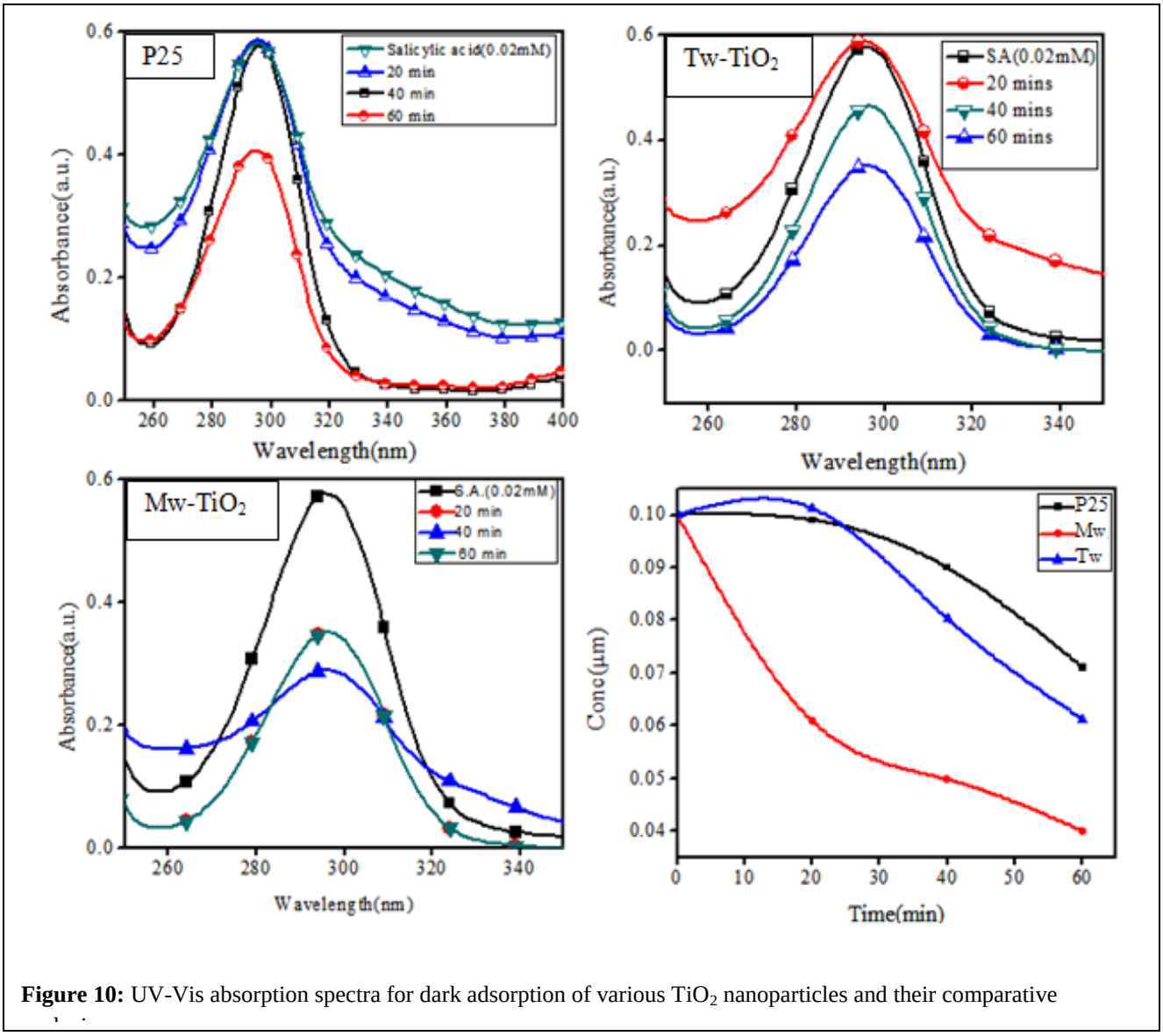

Figure 10: UV-Vis absorption spectra for dark adsorption of various TiO_2 nanoparticles and their comparative

4.4.2 Size and shape effect on Photodegradation:

The figure 11 shows the photodegradation of salicylic acid (0.02 mM) under the influence of various shapes of TiO_2 catalyst under UV irradiation for 2 hrs.The salicylic acid shows $\pi \rightarrow \pi^*$ transitions on irradiation of UV light. The characteristic band at 295 nm in salicylic acid is due to the aromatic ring and it mineralizes to smaller intermediates under UV irradiation. The photodegradation is highly enhanced when the catalyst used is Mw-TiO_2 since the area exposed for surface activity is largely increased as compared to those for Mw-TiO_2 and P25 TiO_2. Figure

11 clearly depicts the fastest degradation in case of Mw-TiO_2 followed by Tw-TiO_2 and then P25. This is due to the elongated surface and more number of active sites available for the adsorption process in case of the Mw-TiO_2 while the Tw-TiO_2 have still lesser area so it clearly gives the photoactivity of the various catalyst and their concentration time graph shows almost equal degradation for the first 20 min i.e., 0.6 µmols for Mw-TiO_2 and P25 TiO_2 and 0.8 µmols for Tw-TiO_2 but exponential decrease is observed for Mw-TiO_2 in the next 20 min interval to 0.09 µmols while it also showed substantial decrease in concentration for Tw-TiO_2 at 0.04µmols while P25 showed concentration of 0.06 µmols. It has been observed from figure 11 that the rate follows pseudofirst order reaction.

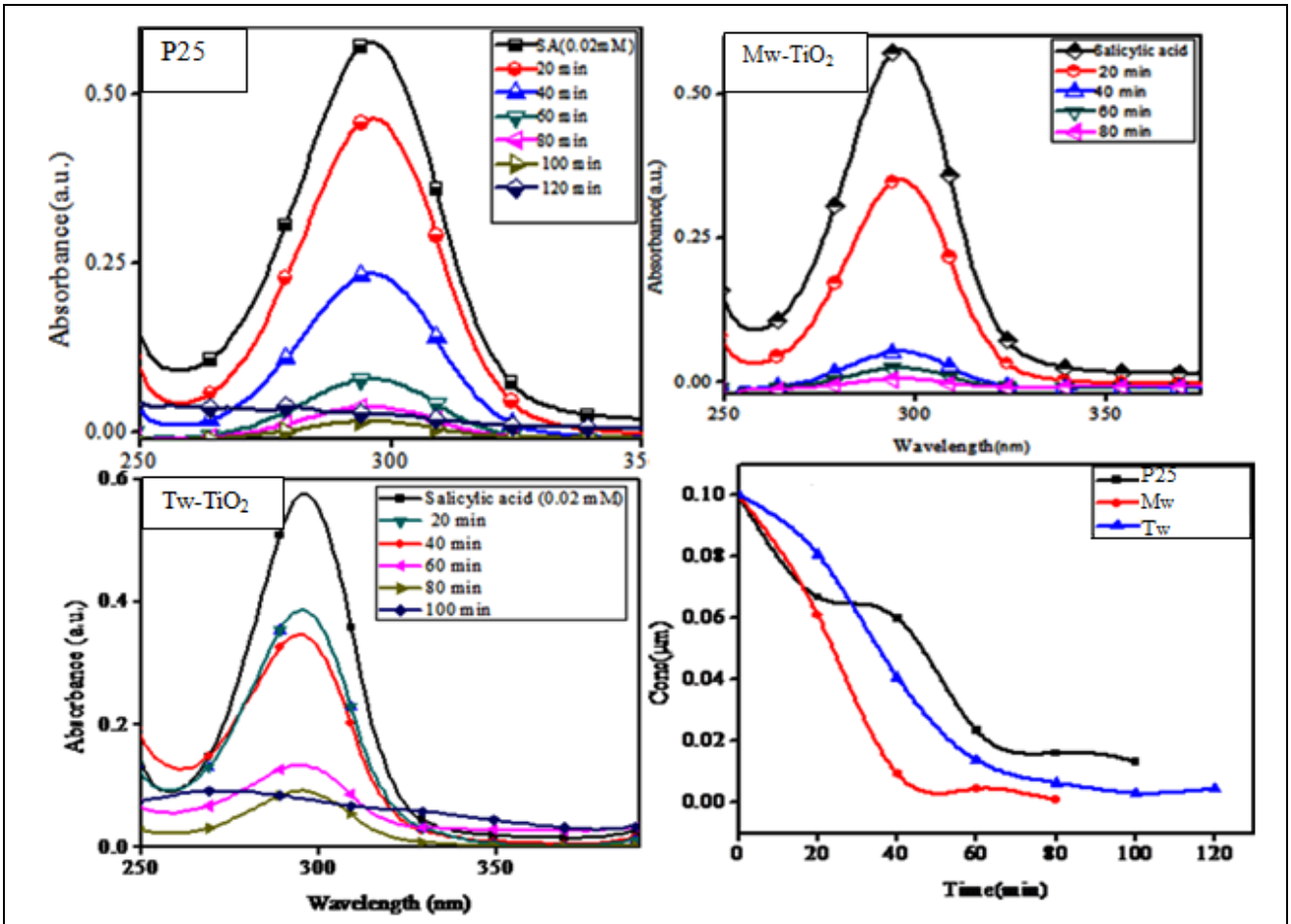

Figure 11: UV-Vis spectra for photodegradation for various titania nanoparticles and their comparative analysis.

4.5 Gas Chromatography:

The amount of CO_2 produced in the reaction process is quantified by Gas Chromatography. The figure 13 illustrates CO_2 evolution of different photocatalyst under prolong UV irradiation. It was observed that complete photodegradation of salicylic acid occurs in 2 hours with Mw-TiO_2 showing maximum CO_2 evolution (1.5 µmols) followed by Tw-TiO_2 (0.6 µmols) and then TiO_2 P25 (0.5 µmols). The band for salicylic acid disappears in 80 minutes confirming the appearance of intermediates as shown in the figure 11 and the complete degradation occurs in 2 hours as suggested by the CO_2 evolution curve in figure 13. This suggests the mechanism of photodegradation of shape selective salicylic acid which takes place by various titania nanoparticles is carried out by photogenerated electrons and holes which result in the formation of highly oxidizing species such as hydroxyl and superoxide radicals and evolve simpler molecules such as CO_2.

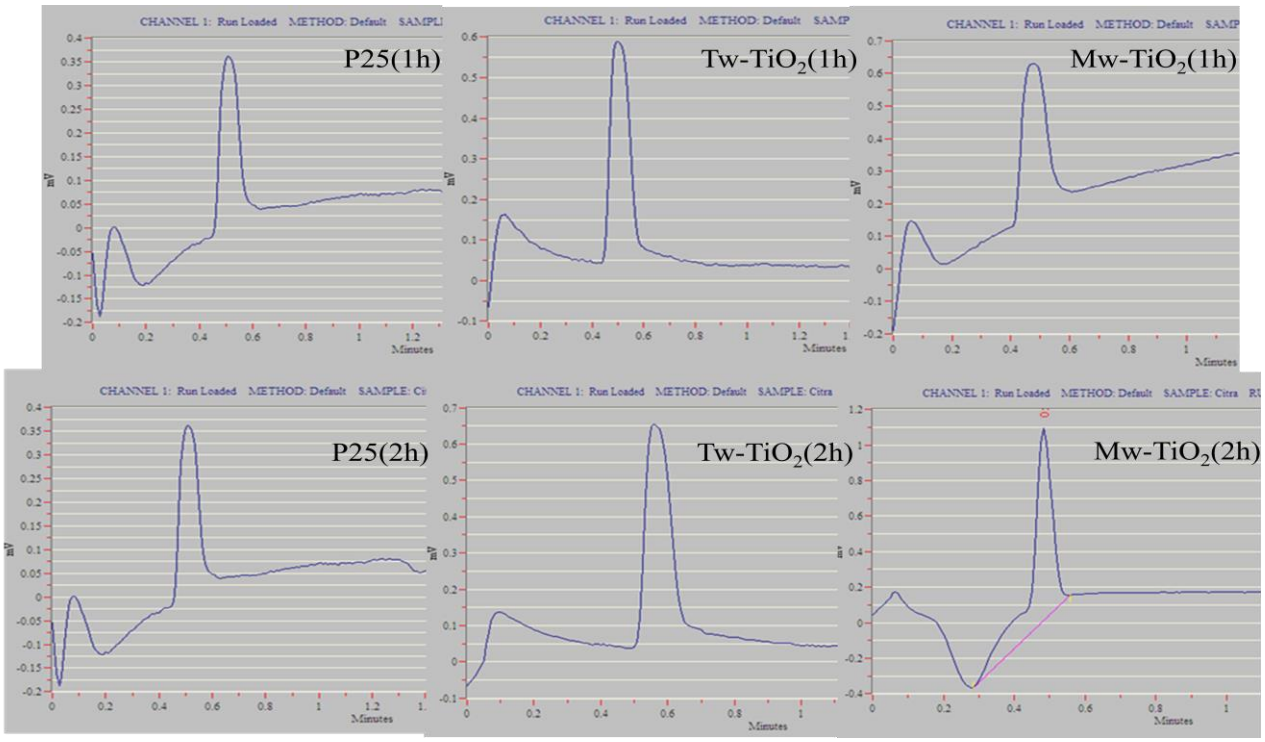

Figure 12: GC graphs of time course evolution of CO_2.

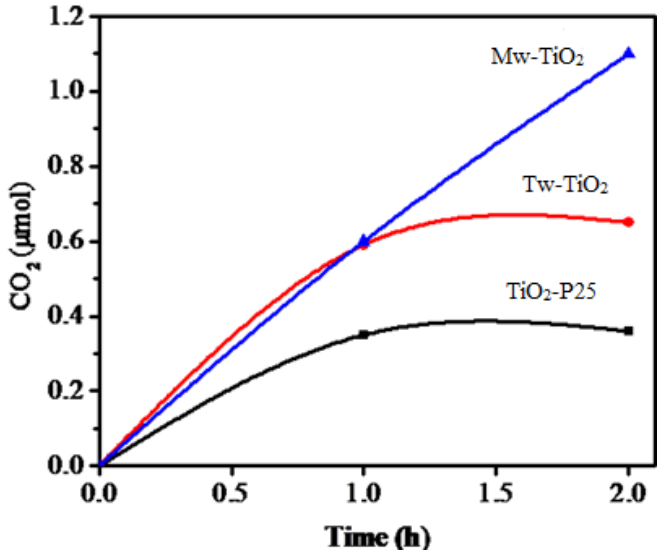

Figure13: CO_2 evolution curve for various titania nanoparticles.

4.6 Biodiesel Characterization:

4.6.1 TLC analysis:

The methyl oleate was identified by generating a TLC and comparing the retention factors with the methyl oleate and oleic acid standards as shown in figure 14. The product obtained from the reaction mixture (b) showed no convergence with the methyl oleate sample (c). Thus no biodiesel formation was reported. Owing to the results shown by TLC it shows that bare TiO_2 is not a suitable catalyst for the methyl oleate formation.

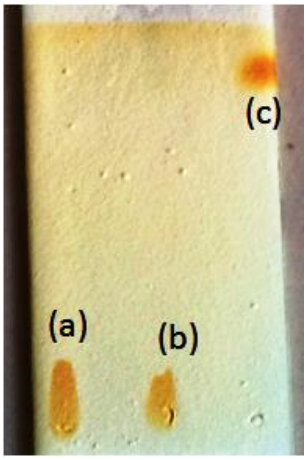

Figure 14: TLC for esterification reaction

4.6.2 FTIR characterization:

The FTIR spectra shown in figure 15, present a comparison among oleic acid, methyl oleate and products obtained upon esterification in presence of various catalysts. Methyl oleate show the characteristic ester carbonyl band at 1750 cm^{-1}, while same band in oleic acid appears at 1706 cm^{-1}. After the reaction acid carbonyl group persist at 1706 cm^{-1} to support that esterification reaction has not taken place. Efforts are in progress to modify the catalyst and reaction condition so that ester formation could be yielded.

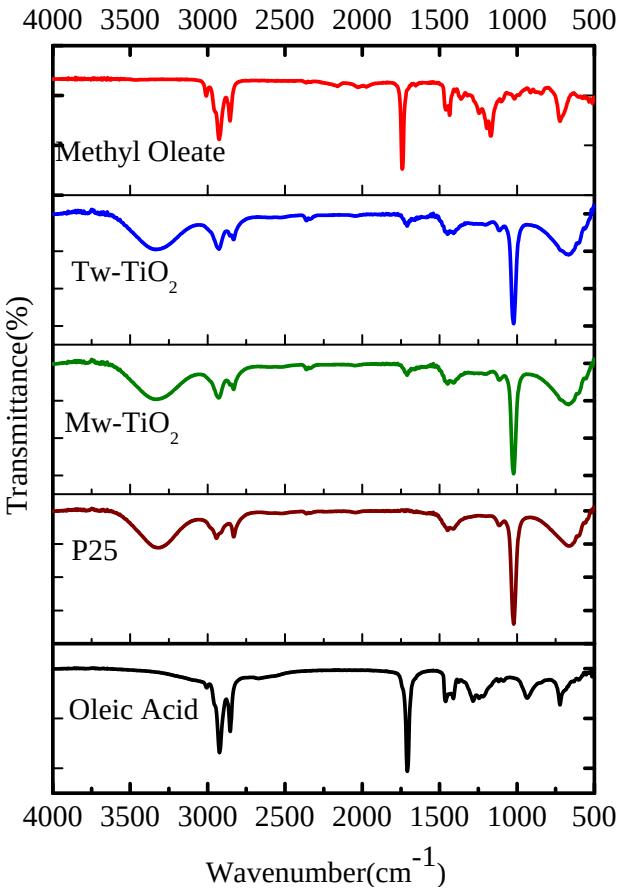

Figure 15: Comparision of FTIR spectrum of oleic acid, methyl oleate and reaction mixture after esterification in presence various catalysts

Chapter 5

Conclusion

In this work TiO_2 catalyst has been prepared under microwave condition and template mediated conventional synthesis. The prepared catalysts were employed for catalyzing two different reactions viz., photodegradation of salicylic acid and esterification of oleic acid. TiO_2 prepared under microwave condition demonstrate better photocatalytic activity than template mediated prepared catalyst. No catalyst was found to be effective for the esterification of oleic acid. Thus TiO_2 prepared under microwave condition has demonstrated better activity owing to the presence of more number of active sites at the elongated surface.

Future Prospects:

The model compound (salicylic acid) was degraded to simpler molecules, however the catalyst can be used to degrade other harmful components such as methylene blue, methyl orange and organic acids such as present in waste waters and can be used for environmental remediation.

Ongoing Research:

The bare titania nanoparticles was not found effective for the esterification of oleic acid. Efforts are in progress to improve the TiO_2 activity by impregnating it with other metals (e.g., alkali metals).

REFERENCES

[1] Zhang, X.; Qin, J.; Xue, Y.; Yu, Zhang, Wang, L.; Liu, R. Effect of aspect ratio and surface defects on the photocatalytic activity of ZnO nanorods. *Sci. Rep.* **2014**, *4596.4*, 1-8.

[2] Pare, B.; Jonnalagadda, S.B.; Tomar, H.; Singh, P.; Bhagwat, V.W. ZnO assisted photocatalytic degradation of acridine orange in aqueous solution using visible irradiation. *Desalination,* **2008**, *232.1,* 80-90.

[3] Hu, J. S.; Ren, L. L. ; Guo, Y. G. ; Liang, H. P. ; Cao A. M, Wan, L.J.; Chun, L. B. Mass production and high photocatalytic activity of ZnS nanoporous nanoparticle. *Angew. Chem. Int. Ed.* **2005**, *117.8,* 1295-1299.

[4] Zhang, J.; Yu, J.; Zhang, Y.; Li, Q.; Gong, J. R, Visible light photocatalytic H_2-production activity of CuS/ZnS porous nanosheets based on photoinduced interfacial charge transfer. *Nano Lett.* **2011**, *11.1,* 4774-4779.

[5] Kuwabata, S.; Nishida, K.; Tsuda, R.; Inoue, H.; Yoneyama, H. Photochemical reduction of carbon dioxide to methanol using ZnS microcrystallite as a photocatalyst in the presence of methanol dehydrogenase. *J. Electrochem. Soc.* **1994**, *141.6*, 1498-1503.

[6] Kalbacova, M.; Macak, J. M.; Stein, F. S., Mierke, C. T.; Schmuki, P. TiO_2 nanotubes: photocatalyst for cancer cell killing**.** physica status *solidi (RRL)-Rapid Research Letters.* **2008**, *2.4*, 194-196.

[7] Lin, W. C.; Yang, W. D.; Huang, L.; Wu, T. S.; Chung, Z. J. Hydrogen Production from Methanol/Water Photocatalytic Decomposition Using Pt/TiO_2 Catalyst. *Energy Fuels.* **2009**, *23.4*, 2192-2196.

[8] Chen, L. C.; Chou, T. C. Photodecolorization of methyl orange using silver ion modified TiO_2 as photocatalyst. *Ind. Eng. Chem. Res.* **1994**, *33.6*, 1436-1443.

[9] Matos, J.; Garcia, A.; Cordero, T.; Chovelon, J. M.; Ferronato, C. Eco-friendly TiO_2–AC photocatalyst for the selective photooxidation of 4-chlorophenol. *Catal. Lett.* **2009**, *130.3-4*, 568-574.

[10] Ishikawa, Y.; Matsumoto, Y.; Nishida, Y.; Taniguchi S.; Watanabe, J. Surface treatment of silicon carbide using TiO_2 (IV) photocatalyst. *J. Am. Chem. Soc.* **2003**, *125.21*, 6558-6562.

[11] Kim, J.; Lee, C. W.; Choi,W. Platinized WO_3 as an environmental photocatalyst that generates OH radicals under visible light. *Env. Sci & tech.* **2010**, *44.17*, 6849-6854.

[12] Chen, D.; Ye, J. Hierarchical WO_3 hollow shells: dendrite, sphere, dumbbell, and their photocatalytic properties." *Adv. Func. Mat.***2008,** *18.13*, 1922-1928.

[13] Lam, K. M.; Lee, K. T.; Mohamed, A. R. Homogeneous, heterogeneous and enzymatic catalysis for transesterification of high free fatty acid oil (waste cooking oil) to biodiesel: a review.*Biotech. Adv.* **2010**, *28.4*, 500-518.

[14] Antczak, S. M. Enzymatic biodiesel synthesis–key factors affecting efficiency of the process. *Ren. Enr.* **2009**, *34.5*, 1185-1194.

[15] Kaur, M.; Ali, A. Lithium ion impregnated calcium oxide as nano catalyst for the biodiesel production from karanja and jatropha oils. *Ren. Enr.* **2011**, *36.11*, 2866-2871.

[16] Chen, X.; Mao, S. S. Titanium dioxide nanomaterials: synthesis, properties, modifications, and applications. *Chem. Rev.* **2007** ,*107.7*, 2891-2959.

[17] Munusamy**, S.**; Aparna, R.S.L. ; Prasad, R.G.S.V. Photocatalytic effect of TiO_2 and the effect of dopants on degradation of brilliant green. *Sus. Chem. Proc.* **2013**, *1.1*, 1-8.

[18] Rodgher, V. Photocatalytic degradation of malic acid using a thin coated TiO_2-film: Insights on the mechanism of photocatalysis. *AIChE. J.* **2014,** *60.9*, 3286-3299.

[19] Turki, A. Design of TiO_2 nanomaterials for the photodegradation of formic acid–Adsorption isotherms and kinetics study. *J. Photochem. And Photobio.A: Chem.* **2014** , *279*, 8-16.

[20] Wen, Z. Biodiesel production from waste cooking oil catalyzed by TiO_2–MgO mixed oxides. *Biores. Tech.* **2010**, *101.24*, 9570-9576.

[21] Chen, L. X. XAFS studies of surface structures of TiO_2 nanoparticles and photocatalytic reduction of metal ions. *The J. of Phy. Chem. B.* **1997**, *101.50*, 10688-10697.

[22] Thompson, T. L.; Yates, J. T. Surface science studies of the photoactivation of TiO_2 new photochemical processes. *Chem. Rev.* **2006,** *106.10*, 4428-4453.

[23] Xingtao, J. Microwave-assisted synthesis of anatase TiO_2 nanorods with mesopores. *Nanotech.* **2007,** *18.7*, 075602.

[24] Damato, T. C.; Caio, C.S.; Pedro H.C. A facile approach to TiO2 colloidal spheres decorated with Au nanoparticles displaying well-defined sizes and uniform dispersion. *Lang.* **2013**, *29.5*, 1642-1649.